

Resonant behavior of the $^{24}\text{Mg}(^{16}\text{O}, ^{12}\text{C})^{28}\text{Si}^*$ ($6.4 \leq E_x \leq 10$ MeV) reaction

S. J. Sanders, C. Olmer,* D. F. Geesaman, W. Henning, D. G. Kovar, M. Paul,[†] and J. P. Schiffer

Argonne National Laboratory, Argonne, Illinois 60439

(Received 16 June 1980)

Excitation functions have been measured for the $^{24}\text{Mg}(^{16}\text{O}, ^{12}\text{C})^{28}\text{Si}$ reaction populating states in ^{28}Si with $6.4 \leq E_x \leq 10$ MeV over the energy range $24 \leq E_{\text{c.m.}} \leq 36$ MeV. At each incident beam energy, cross sections were measured at three angles over the range $17^\circ \leq \theta_{\text{c.m.}} \leq 21^\circ$. More complete angular distributions with $10^\circ \leq \theta_{\text{c.m.}} \leq 50^\circ$ were measured at $E_{\text{c.m.}} = 30.5$ and 32.6 MeV. Resonance-like structures are observed in the excitation functions and strongly correlate with those seen previously at forward angles for the $^{24}\text{Mg}(^{16}\text{O}, ^{12}\text{C})^{28}\text{Si}(\text{g.s.})$ transition. Estimates are made for the partial decay widths of the resonance at $E_{\text{c.m.}} = 30.8$ MeV to the excited states in ^{28}Si . Using different background assumptions, between 5% and 40% of the total width of this resonance can be attributed to $^{12}\text{C} + ^{28}\text{Si}^*$ ($E_x < 10$ MeV) decays.

[NUCLEAR REACTIONS $^{24}\text{Mg}(^{16}\text{O}, ^{12}\text{C})^{28}\text{Si}^*$ ($6.4 \leq E_x \leq 10$ MeV); $24 \leq E_{\text{c.m.}} \leq 36$ MeV; measured $\sigma(E, \theta)$; DWBA analysis; deduced partial widths.]

INTRODUCTION

Resonance-like features have now been observed in the excitation functions for a large number of heavy-ion systems. The resonance behavior appears most pronounced for systems involving "alpha-particle" nuclei (i.e., ^{12}C , ^{16}O , ^{20}Ne , ^{24}Mg , and ^{28}Si) for both target and projectile, although the significance of this observation is not yet clear. One of the lightest systems exhibiting heavy-ion resonance behavior, the $^{12}\text{C} + ^{12}\text{C}$ system, is probably the most thoroughly studied. Cormier *et al.*¹ have shown that the total inelastic $^{12}\text{C} + ^{12}\text{C}(2^+)$ and mutual inelastic $^{12}\text{C}(2^+) + ^{12}\text{C}(2^+)$ yields above the Coulomb barrier exhibit strong, correlated structures with width $\Gamma_{\text{tot}} \sim 1-3$ MeV and spaced several MeV apart. The large partial decay widths which they estimate for these channels lead them to suggest a possible quasimolecular origin. Similar resonance features are observed with 180° elastic and inelastic measurements for $^{12}\text{C} + ^{28}\text{Si}$ and $^{16}\text{O} + ^{24}\text{Mg}$ scattering^{2,3} as well as for the reactions $^{24}\text{Mg}(^{16}\text{O}, ^{12}\text{C})^{28}\text{Si}(0^+, \text{g.s.})$ and $(2^+; 1.78 \text{ MeV})$.^{4,5} In contrast to the $^{12}\text{C} + ^{12}\text{C}$ system, however, only a small fraction (<15%) of the decay width for the common ^{40}Ca compound system resonance can be attributed to these elastic and low-lying reaction channels. (This estimate is derived using the resonance parameters obtained in Ref. 5, with the additional assumption of pure resonance character for the elastic, inelastic, and transfer reaction 180° excitation functions presented in Refs. 2 and 3.) Mapping out the remainder of the decay strength should prove to be valuable in understanding the underlying nature of these structures.

The marked similarities in the forward-angle excitation functions for the ground state and first-

excited 2^+ level of ^{28}Si as populated in the $^{24}\text{Mg}(^{16}\text{O}, ^{12}\text{C})^{28}\text{Si}$ reaction support the search for additional resonance decay strength to states at higher excitation energy in ^{28}Si . Peng *et al.*⁶ have shown that at the energies of interest these excited states are more strongly populated than either the ground or first-excited states. Therefore, excitation functions at forward angles were measured for the strongly populated doublet at 6.9 MeV ($J^\pi = 3^- + 4^+$), the level at 9.7 MeV (5^-), as well as for the total yield to levels with $6.4 \leq E_x \leq 10$ MeV. These excitation functions span the energy range $24 \leq E_{\text{c.m.}} \leq 36$ MeV. More extensive angular distributions than used for the excitation functions were measured at $E_{\text{c.m.}} = 30.5$ and 32.6 MeV.

EXPERIMENTAL METHOD AND DATA REDUCTION

The measurements were performed using the Argonne National Laboratory FN Tandem accelerator. The experimental method was described in Ref. 5 and will only be summarized here. Particle detection and identification of the outgoing ^{12}C ions from the $^{24}\text{Mg}(^{16}\text{O}, ^{12}\text{C})^{28}\text{Si}^*$ reaction were accomplished with an Enge split-pole magnetic spectrograph using a gas ionization chamber, focal plane detector. Self-supporting targets of isotopically pure ^{24}Mg (>99.9% enrichment) and of $\sim 70 \mu\text{g}/\text{cm}^2$ areal density were used. (This areal density corresponds to an energy spread of between 290 and 360 keV for the ^{16}O beam.) The data were normalized using the elastic scattering yields measured in a monitor detector located at $\theta_{\text{lab}} = 17.3^\circ$.

Figure 1 shows an energy spectrum of the outgoing ^{12}C ions for the $^{24}\text{Mg}(^{16}\text{O}, ^{12}\text{C})^{28}\text{Si}$ reaction at $\theta_{\text{lab}} = 13.5^\circ$ and $E_{\text{lab}} = 44.7$ MeV. Dominating this

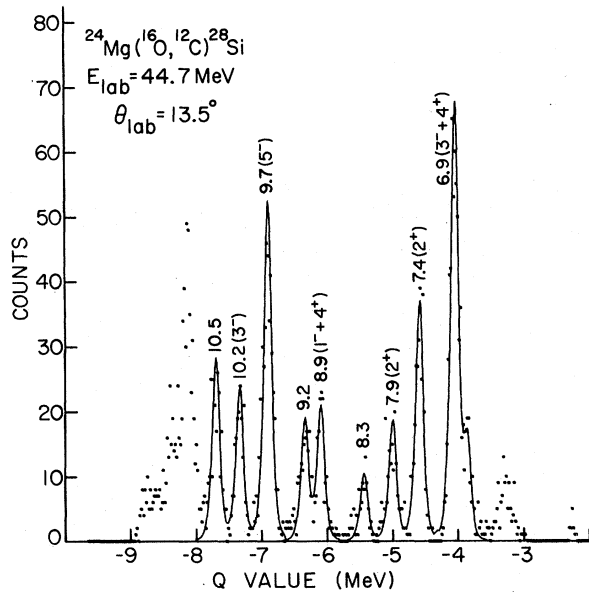


FIG. 1. Energy spectrum for ^{12}C ions from the $^{24}\text{Mg}(^{16}\text{O}, ^{12}\text{C})^{28}\text{Si}$ reaction at $E_{\text{lab}} = 44.7$ MeV and $\theta_{\text{lab}} = 13.5^\circ$. Noted are the energies of known levels in ^{28}Si . The curves are the results of the fitting procedure described in the text.

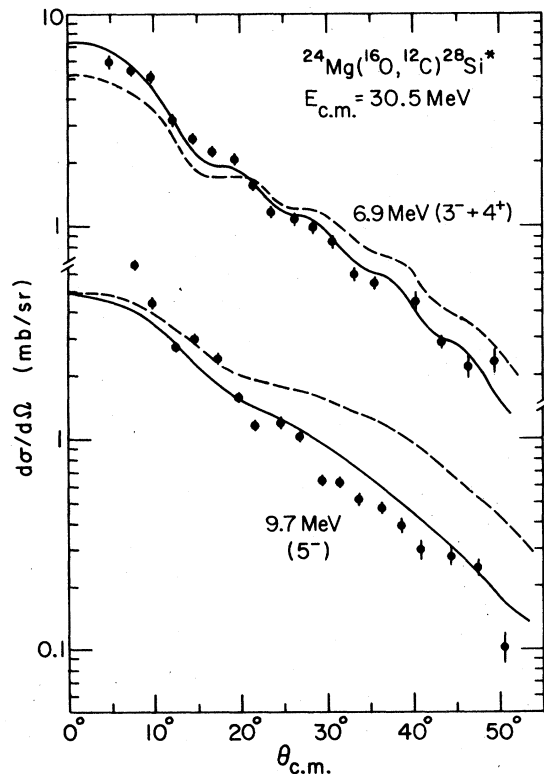


FIG. 2. Angular distribution $E_{\text{c.m.}} = 30.5$ MeV for the 6.9 MeV doublet, and the state at 9.7 MeV in ^{28}Si . The dashed and solid curves are DWBA calculations using potentials A and B, respectively; the 6.9 MeV calculation assumes a 3^- final state.

spectrum are transitions to the levels at $E_x = 6.9$ and 9.7 MeV. The yields for these levels were obtained by fitting the data with a fixed, empirically determined reference-peak line shape. The resulting fits to a number of states in ^{28}Si between 6.4 and 11 MeV are shown in the figure. Although many states are resolved cleanly in this spectrum, the present analysis was limited to the two strongest peaks, and the total yield for $6.4 \leq E_x \leq 10$ MeV. The yields to the more weakly populated states are likely to show a greater sensitivity to carbon and oxygen contaminant yields and therefore were not individually extracted.

Angular distributions for the transitions to the 6.9 and 9.7 MeV levels at $E_{\text{c.m.}} = 30.5$ and 32.6 MeV are shown in Figs. 2 and 3. The angular distributions are found to be relatively featureless with a monotonic decrease in cross section as a function of angle. Except for an overall scaling factor, the angular distributions are also quite similar at the two energies for the respective states. These features suggest that the energy dependence of the total yields can be represented by an excitation function for the yields over a limited angular

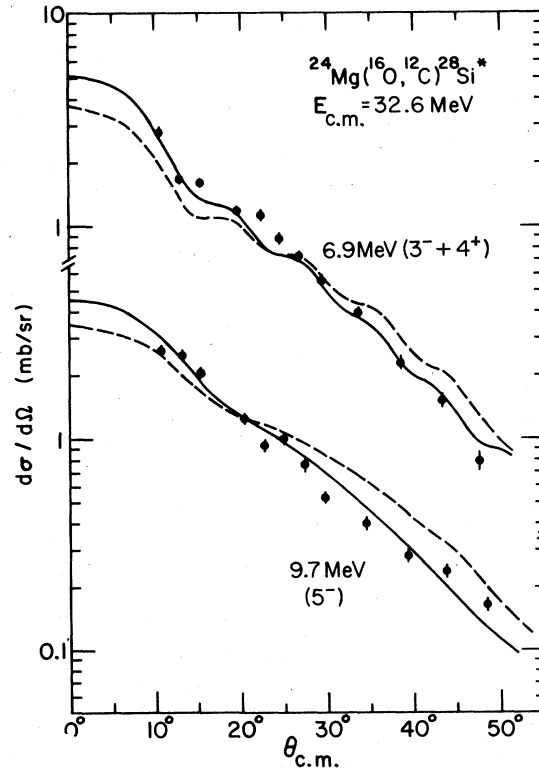


FIG. 3. Angular distributions at $E_{\text{c.m.}} = 32.6$ MeV for the 6.9 MeV doublet, and the state at 9.70 MeV in ^{28}Si . The dashed and solid curves are DWBA calculations using potentials A and B, respectively; the 6.9 MeV calculation assumes a 3^- final state.

range.

Excitation functions were measured for the 6.9-MeV doublet, the 9.7-MeV state, and the yield to all of the states in ^{28}Si in the excitation energy region $6.4 \leq E_x \leq 10$ MeV by measuring yields at three angles, spaced approximately 1.5° apart in the laboratory frame, near $\theta_{\text{lab}} = 12^\circ$ ($\theta_{\text{c.m.}} \sim 19^\circ$). These excitation functions are plotted in Fig. 4 with the previously published 0° excitation function for the ground-state transition.⁴ For the two individual levels the center-of-mass sections integrated between $17^\circ \leq \theta_{\text{c.m.}} \leq 21^\circ$ are plotted. (This angular range was chosen in analogy to the earlier measurement of the ground-state excitation function⁴ where the angular distributions were found to be highly oscillatory and three close angles were chosen to establish the magnitude of the third maximum of the angular distribution. As it turned out, the structureless angular distributions for the higher excited states would not have required the

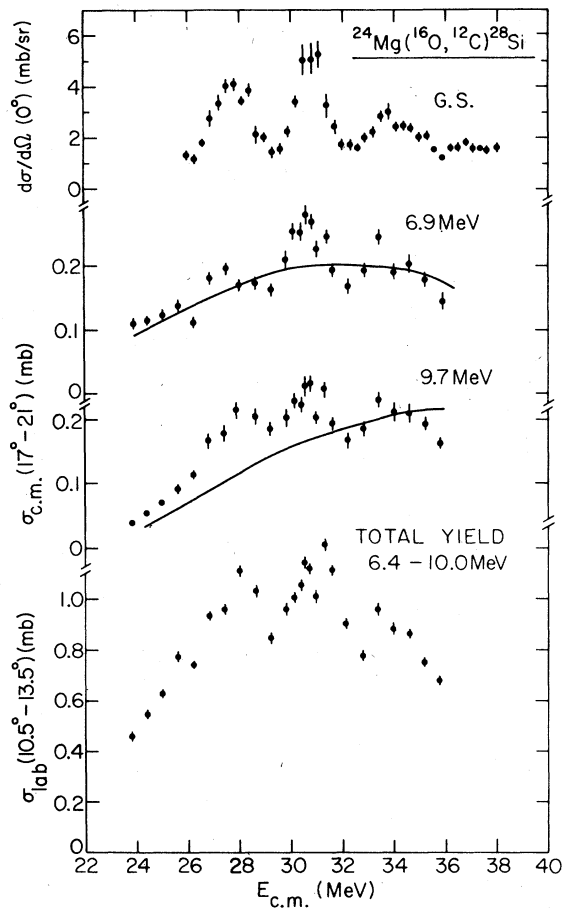


FIG. 4. Excitation functions for states in ^{28}Si populated with the $^{24}\text{Mg}(^{16}\text{O}, ^{12}\text{C})^{28}\text{Si}$ reaction. The ground state excitation function is from Ref. 4 (with the energies corrected as in Ref. 5). The curves are the results of DWBA calculations using potential B.

three close angle measurements.) A center-of-mass conversion is not possible for the total yields to the excited states, and hence the integrated laboratory cross section for $10.5^\circ \leq \theta_{\text{lab}} \leq 13.5^\circ$ is plotted as a function of the incident center of mass energy.

DISTORTED-WAVE BORN APPROXIMATION (DWBA) ANALYSIS

Several analyses of the $^{24}\text{Mg}(^{16}\text{O}, ^{12}\text{C})^{28}\text{Si}$ reaction have employed the DWBA method. Erskine *et al.*⁷ have studied the transitions to the ^{28}Si ground- and first-excited states at $E_{\text{lab}} = 56$ MeV. In later, more extensive studies by Peng *et al.*,⁶ the transitions to a number of low-lying levels in ^{28}Si with $E_x < 10$ MeV were analyzed. (^{28}Si becomes unbound to alpha-particle decay at 9.98 MeV.) The earlier results may be used to establish a reference point from which the observed resonance behavior can be better appreciated. In this section, we discuss those features of the data which can be understood with the nonresonant DWBA theory. Optical potentials quoted in Refs. 6 and 7 were used here and are tabulated in Table I as potentials A and B. The DWBA calculations were made using the code PTOLEMY.⁸

It is assumed in the DWBA calculations that the four nucleons (two protons and two neutrons) are transferred in a relative $L=0$ configuration. The same optical-model potential parameters are used in both the entrance and exit channels. The angular distribution predictions of potentials A and B (see Table I) for the 6.9 MeV doublet and the 9.7 MeV level are compared in Figs. 2 and 3. As in Ref. 6, a pure 3^- configuration is assumed for the doublet. The calculated curves have been normalized to the data. Potential B is found to reproduce the general behavior of the angular distributions quite well at both energies, while potential A does not predict a sufficiently rapid falloff with angle.

Even though potential B reproduces the shape of the angular distributions, the observed energy dependence of the yields is *not* predicted by the DWBA calculation. This is indicated in Fig. 4 where the curves are the predicted excitation functions, integrated over the same angular range as the experimental data, using potential B. The curves have been arbitrarily normalized to the data. Although the overall trend of the excitation functions can be understood in a DWBA framework, the narrow resonance-like structures are not reproduced. Even for the limited angular range employed, the predicted excitation functions vary slowly with energy and show no evidence for the structures seen in the measured excitation functions.

TABLE I. Optical model parameter sets used in DWBA calculations. The optical potential $V(r)$ is given in terms of the listed parameters by the following expressions: $V(r) = -V_0 f(r, R_r, a_0) - iW_0 f(r, R_i, a_{i0})$, $R_r = r_0(A_1^{1/3} + A_2^{1/3})$, $R_i = r_{i0}(A_1^{1/3} + A_2^{1/3})$, $f(r, R, a) = [1 + \exp[(r - R)/a]]^{-1}$.

| | V_0 (MeV) | r_0 (fm) | a_0 (fm) | W_0 (MeV) | r_{i0} (fm) | a_{i0} (fm) | r_{c0} (fm) | Ref. |
|---|----------------|---------------|---------------|----------------|------------------|------------------|------------------|------|
| A | 37 | 1.35 | 0.404 | 78 | 1.290 | 0.174 | 1.2 | 7 |
| B | 35.286 | 1.307 | 0.4926 | 19.67 | 1.242 | 0.204 | 1.307 | 6 |

RESONANCE CONSIDERATIONS

The inability of a conventional application of the DWBA formalism to describe the resonance features was also noted for the ground-state transition in Ref. 5. There a simple characterization of the ground-state excitation function was developed in terms of a few isolated Breit-Wigner resonances added to a nonresonant direct-reaction (DWBA) background. The structure at $E_{c.m.} = 30.8$ MeV was suggested as manifesting an isolated resonance in the ^{40}Ca compound system at an excitation energy of 47.2 MeV and having spin $J = 23$ and total width $\Gamma_{\text{tot}} \sim 800$ keV. Using these parameters, the partial width products $\Gamma_\alpha \Gamma'_\alpha$ for transitions to the excited states in ^{28}Si can then be determined from the expression for the total resonance cross section

$$\sigma_{\alpha\alpha'}^{\text{res}}(E) = \pi\lambda^2(2J + 1) \frac{\Gamma_\alpha \Gamma'_\alpha}{(E_0 - E)^2 + \Gamma_{\text{tot}}^2/4},$$

where α and α' denote the entrance and exit channels, respectively. For the excited states with nonzero spin, the coupling of several possible exit-channel angular momenta to each incident partial wave complicates the problem of establishing the direct background based on DWBA calculations. Limits on the resonance cross section can still be obtained, however, using the measured total yield at energies corresponding to maxima and minima of the excitation functions. Denoting the cross section extrema as σ^{max} and σ^{min} , the minimum resonance cross section is obtained by assuming maximum coherent interference of the resonance with the background,

$$\sigma_{\alpha\alpha'}^{\text{res}} \geq \sigma^{\text{max}} + \sigma^{\text{min}} - 2(\sigma^{\text{max}})^{1/2} (\sigma^{\text{min}})^{1/2}.$$

The maximum resonance cross section is then obtained by taking an incoherent background subtraction,

$$\sigma_{\alpha\alpha'}^{\text{res}} \leq \sigma^{\text{max}} - \sigma^{\text{min}}.$$

The cross sections σ^{max} and σ^{min} were derived from the measured angular distributions at $E_{c.m.} = 30.5$ and 32.6 MeV, respectively. Total angle-integra-

ted cross sections were obtained both by fitting these distributions with the corresponding DWBA calculation and by a simple exponential angle dependence. The integrated yields from 0° to 180° obtained by these two methods generally agreed to better than 20% and averaged values, quoted in Table II, were used in our analysis. These extrapolations to backward angles, in principle underestimate the total yields at the resonance energy. From the measured⁸ backward angle yield for the ground-state transition at $E_{c.m.} = 27.8$ MeV, however, this is estimated to be only a 20–30% effect. This would not significantly change the present discussion, and no further correction of the resonance cross section was attempted. Also quoted in Table II are cross sections for the $J^\pi = 2^+$ level in ^{28}Si at 1.78 MeV (using angular distributions measured earlier⁵), and for the total cross section for populating states in ^{28}Si with $6.4 \leq E_x \leq 10$ MeV (assuming energy averaged kinematics). The limits of resonance cross sections and the resulting estimates of partial width products are tabulated in Table II. This table also lists the partial-width product for the ground-state transition as derived from the Breit-Wigner analysis of Ref. 5.

From simple ratios of $\Gamma_\alpha \Gamma'_\alpha$ where the entrance channel width Γ_α cancels out, it is clear that the partial decay widths Γ'_α to the strongly populated excited states are comparable to or greater than that for the ground-state transition. A rough estimate of the entrance-channel width, assuming a pure resonant contribution to the 180° elastic scattering cross section of Ref. 3, yields $\Gamma(^{16}\text{O} + ^{24}\text{Mg}) \sim 22$ keV. Using this value, the widths in the ^{28}Si channels are calculated and tabulated in Table II. Summing these partial widths, it is found that between 5% and 40% of the total resonance width ($\Gamma_{\text{tot}} \sim 800$ keV) for the $E_{c.m.} = 30.8$ MeV structure can be attributed to the low-lying ($E_x < 10$ MeV) levels in ^{28}Si . Although the 6.9 MeV level appears to have the largest single decay width, many of the low-lying ^{28}Si levels are found to contribute in the resonance decay. (The strongly populated 6.8 and 9.7 MeV levels account for only about 65% of the decay width to states between 6.4 and 10 MeV

TABLE II. Decay parameters for resonance at $E_{\text{c.m.}} = 30.8$ MeV into $^{12}\text{C} + ^{28}\text{Si}$ channels. The excitation energies E_x are for ^{28}Si .

| E_x (MeV) | σ^{max} (mb) | σ^{min} (mb) | $\sigma_{\alpha\alpha}^{\text{res}}$ (mb) | $(\Gamma_{\alpha}\Gamma'_{\alpha})^{1/2}$ (keV) | Γ'_{α} ^a (keV) | $\frac{\gamma_{\alpha}^2}{\theta_w^2}$ ^b ($\times 10^{-3}$) |
|-----------------------|-------------------------------|-------------------------------|--|--|--|---|
| g.s. | | | | 8 ^c | 3 | 1 |
| 1.78 | 0.30 | 0.15 | 0.03–0.15 | 6–15 | 2–10 | 1–5 |
| 6.9 | 2.8 | 1.5 | 0.20–1.30 | 18–45 | 14–91 | 16–100 |
| 9.7 | 2.5 | 1.9 | 0.04–0.60 | 8–30 | 3–42 | 10–143 |
| (6.4–10) ^d | 10.2 | 6.7 | 0.37–3.5 | 24–73 | 26–244 | 44–419 |

^a The width for the entrance channel $\Gamma_{\alpha} \approx 22$ keV was deduced from 180° elastic scattering measurements (Ref. 3) for the $^{16}\text{O} + ^{24}\text{Mg}$ system.

^b $\gamma_{\alpha}^2 = \Gamma'_{\alpha}/2P_l$ with $P_l = kR/(F_l^2 + G_l^2)$. The R -matrix radius $R = 1.6(12^{1/3} + 28^{1/3}) = 8.52$ fm was used for these calculations. The reduced widths γ_{α}^2 are calculated assuming the smallest permitted l for a given final state spin S , i.e., $l = J - S$, where J is the resonance spin ($J = 23$), and S is the spin of the residual ^{28}Si state. The Wigner sum rule limit θ_w^2 is given by $\frac{3}{2}\hbar^2/\mu R^2 = 103$ keV.

^c From Ref. 5.

^d Energy averaged kinematics were used. For the reduced width, the penetrability was computed for $l = J - S = 20$.

in ^{28}Si excitation energy.) Also tabulated in Table II are the ratios of the reduced widths γ_{α}^2 to the Wigner sum rule limit θ_w^2 . The reduced widths are calculated assuming a maximum value for the Coulomb penetrability factor P_l which occurs for $l = J - S$ where J is the resonance spin and S is the spin of the residual ^{28}Si state. Within the uncertainties of this analysis the strongly populated states all have similar partial decay widths. This suggests that even higher excited states in ^{28}Si may play a significant role in the resonance decay.

SUMMARY AND CONCLUSIONS

The forward-angle resonance characteristics of the $^{24}\text{Mg}(^{16}\text{O}, ^{12}\text{C})^{28}\text{Si}$ reaction, as reported in Refs. 4 and 5 for the ^{28}Si (g.s.) and first-excited state transitions, are found to be common for transitions to many of the states in ^{28}Si with $E_x < 10$ MeV. Starting with the parameters of Ref. 5 for the $^{40}\text{Ca}^*$ (47.2 MeV; $J = 23$) resonance, the decay widths are deduced for two strongly populated levels in ^{28}Si at 6.9 and 9.70 MeV. Between 5 and 40% of the total decay width for this proposed $J = 23$ resonance can be attributed to decays to states in ^{28}Si with $E_x < 10$ MeV [the ^{28}Si (g.s.) transition accounts for $\sim 0.5\%$ of the total width]. The summed decay width to states in ^{28}Si is therefore found to be comparable to or larger than the $^{16}\text{O} + ^{24}\text{Mg}$ (g.s.) channel width.

It is interesting to note that the states observed to be populated strongly in the $^{24}\text{Mg}(^{16}\text{O}, ^{12}\text{C})^{28}\text{Si}$ reaction are the same states to be excited strongly in (p, p') (Ref. 9) and (π, π') (Ref. 10) scatter-

ing on ^{28}Si . From a recent compilation,¹¹ there are 29 known states in ^{28}Si with $E_x < 10$ MeV. Of these, the two strongest states seen here (at 6.9 and 9.7 MeV) are also the strongest populated states in (p, p') scattering. Three of the four next most strongly populated states here are also the next strongest in (p, p') . The strong states in (p, p') must be the ones that are connected to the ^{28}Si ground state by a simple excitation. The fact that the same states appear strongly in the $^{24}\text{Mg}(^{16}\text{O}, ^{12}\text{C})^{28}\text{Si}$ reaction emphasizes that this reaction favors the same configurations that are closely linked to the ground state of ^{28}Si . A structural link between the resonances and the common configurations in the ground and related states in ^{28}Si is indicated by the observation that the two strongest states are also found to exhaust a dominant part ($\sim 65\%$) of the resonance partial widths for ^{28}Si states in the range $6.4 \leq E_x \leq 10$ MeV.

Although the resonance features are clearly observed in the $^{12}\text{C} + ^{28}\text{Si}^*$ channels, even if one takes the maximum values for the partial widths a substantial fraction ($> 50\%$) of the total width for the state at $E_x(^{40}\text{Ca}) = 47.2$ MeV is unaccounted for. Other channels that are well matched in angular momentum include: excited states of ^{24}Mg , the 2^+ state of ^{12}C , and low-lying states in $^{20}\text{Ne} + ^{20}\text{Ne}$. In addition, the possibility that the full width observed here also includes some spreading width due to unresolved intermediate structure cannot be ignored.

This work was performed under the auspices of the U. S. Department of Energy.

- *Present address: Physics Department, Indiana University, Bloomington, Indiana 47401.
- †Present address: Racah Institute of Physics, The Hebrew University of Jerusalem, Israel.
- ¹T. M. Cormier, J. Applegate, G. M. Berkowitz, P. Braun-Munzinger, P. M. Cormier, J. W. Harris, C. M. Jachcinski, L. L. Lee, Jr., J. Barrette, and H. E. Wegner, *Phys. Rev. Lett.* **38**, 940 (1977); T. M. Cormier, C. M. Jachcinski, G. M. Berkowitz, P. Braun-Munzinger, P. M. Cormier, M. Gai, J. W. Harris, J. Barrette, and H. E. Wegner, *ibid.* **40**, 924 (1978).
- ²J. Barrette, M. J. LeVine, P. Braun-Munzinger, G. M. Berkowitz, M. Gai, J. W. Harris, C. M. Jachcinski, and C. D. Uhlhorn, *Phys. Rev. C* **20**, 1759 (1979).
- ³M. Paul, S. J. Sanders, D. F. Geesaman, W. Henning, D. G. Kovar, C. Olmer, J. P. Schiffer, J. Barrette, and M. J. LeVine, *Phys. Rev. C* **21**, 1802 (1980).
- ⁴M. Paul, S. J. Sanders, J. Cseh, D. F. Geesaman, W. Henning, D. G. Kovar, C. Olmer, and J. P. Schiffer, *Phys. Rev. Lett.* **40**, 1310 (1978).
- ⁵S. J. Sanders, M. Paul, J. Cseh, D. F. Geesaman, W. Henning, D. G. Kovar, R. Kozub, C. Olmer, and J. P. Schiffer, *Phys. Rev. C* **21**, 1810 (1980).
- ⁶J. C. Peng, J. V. Maher, W. Oerlet, D. A. Sink, C. M. Cheng, and H. S. Song, *Nucl. Phys. A* **264**, 312 (1976).
- ⁷J. R. Erskine, W. Henning, D. G. Kovar, L. R. Greenwood, and R. M. DeVries, *Phys. Rev. Lett.* **34**, 680 (1975).
- ⁸Code PTOLEMY, M. H. Macfarlane and S. C. Pieper, Argonne National Laboratory Informal Report No. ANL-76-11 Rev. 1, 1978 (unpublished).
- ⁹G. S. Adams, A. D. Bacher, G. T. Emery, W. P. Jones, R. T. Kouzes, D. W. Miller, A. Picklesimer, and G. E. Walker, *Phys. Rev. Lett.* **38**, 1387 (1977).
- ¹⁰C. Olmer, B. Zeidman, D. F. Geesaman, T.-S. H. Lee, R. E. Segel, L. W. Swenson, R. L. Boudrie, G. S. Blanpied, H. A. Thiessen, C. L. Morris, and R. E. Anderson, *Phys. Rev. Lett.* **43**, 612 (1979).
- ¹¹P. M. Endt and C. van der Leun, *Nucl. Phys. A* **310**, 1 (1978).